DESY 94-025
February 1994

Finite Temperature Effective Potential to Order g^4, λ^2 and the Electroweak Phase Transition

Zoltán Fodor [1] and Arthur Hebecker

Deutsches Elektronen-Synchrotron DESY, Hamburg D-22603, Germany

Abstract

The standard model effective potential is calculated at finite temperature to order g^4, λ^2 and a complete zero temperature renormalization is performed. In comparison with lower order calculations the strength of the first order phase transition has increased dramatically. This effect can be traced back to infrared contributions from typical non-Abelian diagrams and to the infrared behaviour of the scalar sector close to the critical temperature. Several quantities, e.g. surface tension, latent heat and field expectation value are analyzed for an SU(2)-Higgs model and for the full standard model in detail. An explicit formula enabling further analytic or numerical study is presented.

[1] On leave from Institute for Theoretical Physics, Eötvös University, Budapest, Hungary

1 Introduction

Recently it has been clarified that the electroweak phase transition plays an important role for the observed baryon asymmetry of the universe [1] (for a recent review see [2]).

Several approaches have been used to determine the details of the electroweak phase transition. Important results have been obtained by use of 3-dimensional effective theory [3], ϵ-expansion [4, 5] and average action [6]. There is also a growing interest in lattice simulations of the phase transition [7].

Perturbative calculations of the finite temperature effective potential of the standard model have been carried out using the one loop ring summation [8, 9] to order $g^3, \lambda^{3/2}$ (g denotes the gauge-coupling and the top-Yukawa coupling). Two-loop summation has been done to order g^4, λ in [10], in which scalar masses have been neglected with respect to gauge-boson masses, and by use of another approximation in [11].

However, there is a need to extend the work of Arnold and Espinosa [10] to a complete g^4, λ^2-calculation. The analysis of the Abelian Higgs model has shown, that higher order λ-corrections can change the g^4, λ-result for the potential and surface tension significantly [12]. Despite the general scepticism concerning the predictive power of the perturbative results in the Φ^4-theory, note that calculating far enough in the resummed loop expansion the obtained effective potential suggests the correct second order phase transition. For the Z_2-symmetric Φ^4-model one should go to the order λ^2, while for the O(4)-symmetric Φ^4-model even a $\lambda^{3/2}$-calculation is sufficient.

The calculation of the g^4, λ^2-potential for the standard model and its detailed analysis are the main goals of the present paper. A systematic expansion in coupling constants is performed taking into account the effects of infrared divergences [9] and keeping the full dependence on the Higgs field φ, its zero temperature vacuum expectation value v and the temperature T. The effect of the higher order λ-corrections is found to be important for realistic Higgs masses.

The principal method of the calculation, based on the Dyson-Schwinger equation for the derivative $\partial V/\partial\varphi$, is explained in sect. 1 for some general theory containing all the important features of the standard model. Essentially a summation of tadpole diagrams is performed [13]. The application to the standard model is carried out and the renormalization at zero temperature is presented.

In sect. 2 the pure SU(2)-Higgs model is analysed in detail. Using the surface tension and other physical quantities a comparison of the different order calculations is performed. In contrast to the Abelian case, here the g^4, λ-potential suggests a stronger first order phase

transition than the $g^3, \lambda^{3/2}$-potential. Improving the calculation from order g^4, λ to g^4, λ^2 a stronger first order phase transition is obtained for both the Abelian and the non-Abelian case. Of course, this effect questions the reliability of the perturbative approach. The increase of the surface tension is traced back to the infrared features of typical non-Abelian diagrams. The observed numerical importance of the λ-corrections has its roots in the infrared region as well.

The complete standard model results are discussed in sect. 3. The large top quark mass leads to a decrease of the surface tension. Nevertheless, the qualitative picture is the same as for the pure SU(2) case.

After some conclusions in sect. 4 the complete analytic result for the standard model is presented in the appendix.

2 Calculation of the effective potential at finite temperature

2.1 General idea

The effective potential V is calculated using Dyson-Schwinger equations, as described for the Abelian Higgs model in [12]. A similar way of summing the different contributions to V for the Φ^4 theory has been considered in [14].

Consider a general Lagrangian with interaction terms generating 3- and 4-vertices proportional to g^2 and 3-vertices proportional to $g\,k_\mu$. A generic coupling constant g is used as an expansion parameter and k_μ is a momentum variable. Note that this structure is suggested by the standard model Lagrangian where the square root of the scalar coupling $\sqrt{\lambda}$, the Yukawa coupling g_Y, the electroweak gauge couplings g_1, g_2 and the strong gauge coupling g_s play the role of the generic coupling g. Here we give all contributions to the finite temperature effective potential up to order g^4. All calculations are carried out in the imaginary time formalism.

Using the well known technique of Dyson-Schwinger equations the following relation can be obtained for the effective potential

$$-\partial(\mathrm{V}-\mathrm{V}_{\mathrm{tree}})/\partial\varphi = \mathrm{A}+\mathrm{B} \equiv$$

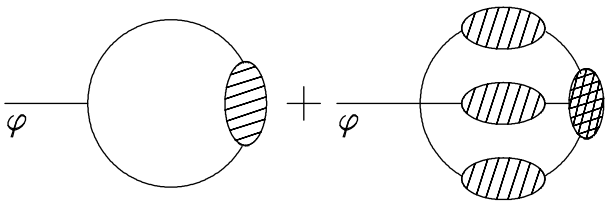

(1)

Here the internal lines represent all particles of the theory and φ is the "shift" of the Lagrangian in the scalar sector. The two different sorts of blobs are full propagator and full 3-vertex respectively. The first term gives

$$A = \mathrm{tr}\, \mathcal{W}(\varphi) \sum\!\!\!\!\!\!\int \frac{dk}{k^2 + m_{tree}^2 + \Pi(k)} \,. \tag{2}$$

In general, mass, self energy and vertex $\mathcal{W}$ are matrices. "tr" denotes the sum over the suppressed indices. For vector particles the self energies are different for the longitudinal and transverse part. They can be calculated using the corresponding projection operators (see [15, 16]). The φ-dependence of the propagators is obvious.

The Dyson-Schwinger equation for $\Pi(k)$, to the order needed in this calculation, reads

$-\Pi(\mathrm{k}) = -(\Pi_\mathrm{a}(\mathrm{k}) + \Pi_\mathrm{b}(\mathrm{k})) \equiv$ 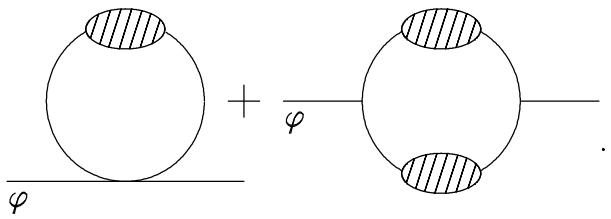 (3)

In the following the indices 2 and 3 denote the contributions of order g^2 and g^3 respectively. The tadpole part of the self energy can be written as

$$\Pi_a(k) = \Pi_{a2} + \Pi_{a2}(k) + \Pi_{a3} + \cdots \qquad \text{with} \quad \Pi_{a2}(0) = 0 \,. \tag{4}$$

In the standard model the only nonvanishing $\Pi_{a2}(k)$-contribution is the longitudinal self energy of a non-Abelian gauge boson. It is introduced by the corresponding projection operator when applied to the four vector vertex. The momentum dependence of the third order term disappears if $k_0 = 0$, thus in the order we are calculating it can be neglected.

The other part of the self energy, $\Pi_b(k)$, has no contribution of order g^2 for scalars. Nevertheless, for gauge particles those terms do appear. The leading order momentum independent part of $\Pi_b(k)$ will be called Π_{b2}.

Using these definitions and introducing the corrected mass term m^2,

$$m^2 = m_{tree}^2 + \Pi_{a2} + \Pi_{b2} \quad , \tag{5}$$

equation (2) can be written as

$$A = \mathrm{tr}\, \mathcal{W}(\varphi) \sum\!\!\!\!\!\!\int \frac{dk}{k^2 + m^2 + \Pi_{a2}(k) + \Pi_{a3} + \Pi_b(k) - \Pi_{b2}}$$

$$= \mathrm{tr}\,\mathcal{W}(\varphi')\sum\!\!\!\!\!\!\int dk \left(\frac{1}{k^2+m^2+\Pi_{a2}(k)} - \frac{1}{k^2+m^2}\Pi_{a3}\frac{1}{k^2+m^2} \right.$$
$$\left. + \frac{1}{k^2+m^2}\Pi_{b2}\frac{1}{k^2+m^2} - \frac{1}{k^2+m^2}\Pi_b(k)\frac{1}{k^2+m^2} \right). \qquad (6)$$

Here the second equality is obtained by expanding the integrand in g. This is best seen by considering the $k_0 = 0$ and $k_0 \neq 0$ parts separately.

Observe that in term B of (1) the vertex need not be corrected to obtain the full g^4-result. Inspection of the last term of (6) and term B of (1) shows that their sum is equal to the derivative $-\partial V_\ominus/\partial\varphi$, where $-V_\ominus$ represents the sum of all two-loop diagrams of the type shown in fig. 1.a (setting sun diagrams).

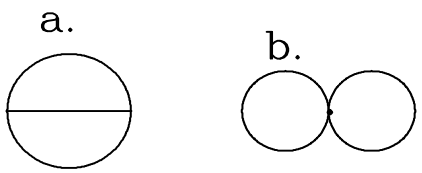

Fig.1 Typical two loop diagrams

With the definitions

$$V_R = -\int^\varphi d\varphi' \mathrm{tr}\,\mathcal{W}(\varphi')\sum\!\!\!\!\!\!\int dk \left(\frac{1}{k^2+m^2+\Pi_{a2}(k)} + \frac{1}{k^2+m^2}\Pi_{b2}\frac{1}{k^2+m^2} \right), \qquad (7)$$

$$V_z = \int^\varphi d\varphi' \mathrm{tr}\,\mathcal{W}(\varphi')\sum\!\!\!\!\!\!\int dk \frac{1}{k^2+m^2}\Pi_{a3}\frac{1}{k^2+m^2}, \qquad (8)$$

the potential can be given in the form

$$V = V_{tree} + V_\ominus + V_z + V_R\,. \qquad (9)$$

Note that V_z can be identified as the sum of all terms bilinear in masses coming from two-loop diagrams of the type shown in fig. 1.b.

Denoting by V_3 the sum of the tree level potential and the g^3-order part of V_R and calling V_4 the fourth order corrections of V_R,

$$V_3 + V_4 = V_{tree} + V_R, \qquad (10)$$

the following final formula is obtained :

$$V = V_3 + V_4 + V_\ominus + V_z. \qquad (11)$$

It is worthwhile to mention the differences between the method given here and the one presented in [10]. One advantage of our approach is the absence of thermal counterterms.

The other one is the fact that no different treatment of zero and nonzero Matsubara frequency modes is needed. Nevertheless, performing the rather tedious calculation using both methods the above mentioned advantages turned out to be marginal.

2.2 Standard model calculation

To fix our notation the essential parts of the Lagrangian are given

$$\mathcal{L} = \mathcal{L}_{Higgs} + \mathcal{L}_{gauge} + \mathcal{L}_{fermion} + \mathcal{L}_{Yukawa}. \tag{12}$$

Defining the covariant derivative as

$$D_\mu = \partial_\mu + ig_1 \frac{Y}{2} B_\mu + ig_2 \frac{\tau^a}{2} W_\mu^a \tag{13}$$

the fermionic and gauge parts are unambiguous. The Higgs contribution reads

$$\mathcal{L}_{Higgs} = -|D_\mu \Phi|^2 + \nu |\Phi|^2 - \lambda |\Phi|^4 \quad , \quad \text{where} \quad \Phi = \frac{1}{\sqrt{2}} \begin{pmatrix} \varphi_3 + i\varphi_4 \\ \varphi + \varphi_1 + i\varphi_2 \end{pmatrix} \tag{14}$$

denotes the Higgs doublet. All fermions except the top quark are considered to be massless. The resulting Yukawa Lagrangian reads

$$\mathcal{L}_{Yukawa} = -g_Y \bar{q}_L \tilde{\Phi} t_R \,, \qquad q_L = \begin{pmatrix} t_L \\ b_L \end{pmatrix}, \qquad \tilde{\Phi} = i\tau_2 \Phi^*. \tag{15}$$

The calculation is performed in Landau gauge. To define the potential to the order g^4, λ^2 the formal power counting rule

$$g_1 \sim g_2 \sim g_Y \sim \lambda^{1/2} \tag{16}$$

is used. We assume $\nu = \lambda v^2$ to be of order λ, where v is the zero temperature vacuum expectation value of the scalar field. This expansion in the couplings seems to be natural, since it corresponds to the general structure of the theory, described in the previous subsection. All masses are treated symmetrically as terms of order g. To the given order the full dependence on temperature, order parameter φ and v is kept.

This clarifies the way, how the general considerations of the previous subsection have to be applied to the standard model. The different contributions to $V_\ominus$ are shown in fig. 2. As usual, solid, dashed and wavy lines represent fermion, scalar and vector propagators respectively. In order to make the explicit comparison with the results of [10] easier we follow the labeling of the setting sun diagrams given there

$$V_\ominus = V_a + V_b + V_i + V_j + V_m + V_p. \tag{17}$$

We have included ghost contributions in V_m. V_p is the scalar setting sun contribution not considered in the standard model calculation of [10].

The calculation needed for the temperature dependent masses to order $g^3, \lambda^{3/2}$ is similar to that performed in [9, 16]. With the help of these masses one can evaluate V_4 and V_z in eq. (11). Notice, that working in dimensional regularization the leading order ϵ-dependence has to be kept in the plasma masses, because it gives finite contributions to the order g^4, λ^2 due to one-loop divergences. The scalar integral for $V_\ominus$ can be found in [17]. More complicated diagrams of this type can be reduced to the scalar case as described in [10]. These calculations have to be extended to include all contributions of order g^4, λ^2. After a long but straightforward calculation the explicit formula for the potential in $\overline{\rm MS}$-scheme is obtained. This final result is given in the appendix. Dropping the appropriate terms of V the lower order g^4, λ-result, as it is given by Arnold and Espinosa in [10], can be derived. We have found some minor discrepancies. A careful check of the differences has shown that some misprints[2] in [10] have to be corrected to obtain complete agreement.

We have checked our full g^4, λ^2-result using the method of [10]. Zero Matsubara frequency modes have been resummed and the necessary temperature counterterms have been calculated. The obtained potential is in complete agreement with the one we give in the appendix.

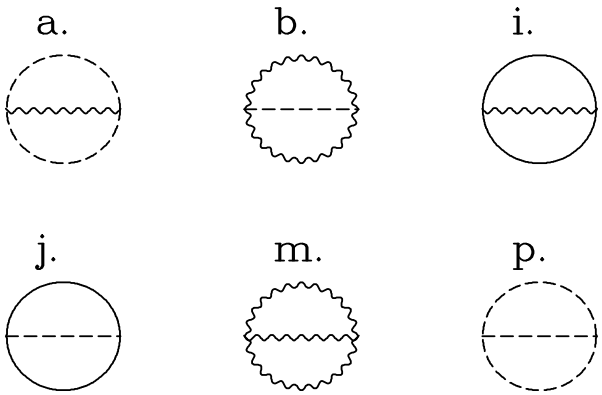

Fig.2 Setting sun diagrams for the standard model

Note, that there are linear φ-terms of fourth order in the couplings present in V_a and V_z. These terms cancel each other, thus ensuring the relation $\lim_{\varphi\to 0} \partial V/\partial\varphi = 0$ for all allowed temperatures. This cancellation is essentially the same effect which leads to a vanishing

[2] σ in eq.(8.2,8.3), eq.(A11) line 9, eq.(A19l), eq.(A19m) line 5, eq.(A19o) line 2, eq.(A25) line 2, eq.(A45)

third order transverse gauge boson mass in the symmetric phase [9], as it can be seen in the contributions of diagrams fig. 6.o and fig. 6.t of [9].

The result of the present paper with the wave function correction term of [18] gives the finite temperature effective action up to order g^4, λ^2.

2.3 Renormalization in the standard model

In case of the standard model it is not possible to avoid the zero temperature renormalization just by setting $\bar{\mu} = 1/\beta$. The reason for that is the large negative $g_Y^4\varphi^4$-term, which dominates over the tree level quartic term. This leads to an $\overline{\text{MS}}$-potential unbounded from below for moderately large top mass and small Higgs mass.

We perform a zero temperature renormalization in the on-shell scheme, as described in [19]. Higgs mass, top quark mass, W- and Z-boson masses and the fine structure constant α are chosen as physical parameters [20]. The physical masses are the poles of the propagators and α is defined in the Thompson limit. A multiplicative renormalization of the coupling constants, the tree level Higgs mass square $-\nu$ and the physical Higgs field is performed. The wave function renormalization of the Higgs field is defined as usual by

$$\delta Z_\varphi = \frac{\partial}{\partial q^2} \mathrm{Re}\, \Pi_\varphi(q^2)\Big|_{q^2=m^2_{\varphi,phys}} . \tag{18}$$

No wave function renormalization is needed for the other fields, because they do not appear in the effective potential. v is defined to be the true vacuum expectation value of the physical Higgs field. Therefore it needs no corrections and no tadpole diagrams have to be considered.

The correction to the electric charge δe is gauge independent [21], as it can be easily checked explicitly using the results of [22]. Therefore in the present calculation the formula for δe from [19] is used. The logarithmic terms with the five light quark masses are treated in the way described in [23], with data from [24], resulting in the vacuum polarization contribution:

$$\mathrm{Re}\,\Pi^{\gamma(5)}_{\mathrm{had}}(M_Z^2) = -0.0282 \pm 0.0009\,. \tag{19}$$

The dependence of the one-loop self energy corrections on the gauge parameters has been calculated in [22] for gauge bosons. Therefore the corrections in Landau gauge, needed here, can be taken from [22, 25]. The self energy corrections for the physical Higgs boson and the top quark can be easily calculated in Landau gauge. Using these quantities the complete zero temperature renormalization of the potential can be done. The result is thereby freed of any dependence on $\bar{\mu}$.

Clearly, the analytic expression of these corrections to the potential is too long to be given here. However, it seems worthwhile to give the numerically most important parts of the corrections, to enable a simplified usage of the analytic result in the appendix. As it has already been mentioned, the main contributions come from the g_Y^4-corrections to parameters of order λ (see also [10]):

$$\delta\lambda = \frac{3g_Y^4}{8\pi^2}\ln\frac{m_t}{\bar{\mu}} \quad , \quad \delta\nu = \frac{3g_Y^4 v^2}{16\pi^2}. \tag{20}$$

Introducing this corrections in all terms in the potential contributing to order λ and using standard model tree level relations to calculate the couplings one obtains a result which is "partially renormalized at zero temperature". The corresponding correction to the $\overline{\text{MS}}$-potential reads

$$\delta V = \frac{\varphi^2}{2}\left(-\delta\nu + \frac{1}{2\beta^2}\delta\lambda\right) + \frac{\delta\lambda}{4}\varphi^4 . \tag{21}$$

As we will see it later (sect.4), the numerical effect of this simplification is not too severe.

3 Results for pure SU(2)-Higgs model

3.1 Effective potential and surface tension

To obtain an understanding of the qualitative effects of higher order corrections we study first the pure SU(2)-Higgs model. In this section the additional U(1)-symmetry and the effect of the fermions are neglected. A discussion of this simplified version may also be useful in view of lattice investigations, which will probably deal with the pure SU(2)-Higgs model in the near future.

The relevant potential can be easily derived from the formulas given in the appendix by performing the limit $g_1, g_Y \longrightarrow 0$ and setting the number of families n_f to zero. Throughout this section standard model values for W-mass and vacuum expectation value v are used, unless stated otherwise : $m_W = 80.22$ GeV and $v = 251.78$ GeV. The parameter $\bar{\mu}$ of dimensional regularization is set to $T = 1/\beta$. This can be justified by the small dependence on the renormalization procedure. The differences between the results obtained in this scheme and in a scheme with on-shell $T = 0$ renormalization are very small. This phenomenon has been observed in the Abelian Higgs model as well [12].

In fig. 3 different approximations of the effective potential at their respective critical temperatures are shown. The potentials to order $g^3, \lambda^{3/2}$ and g^4, λ can be obtained from [8, 9] and [10] respectively. Each approximation suggests a first order phase transition. On

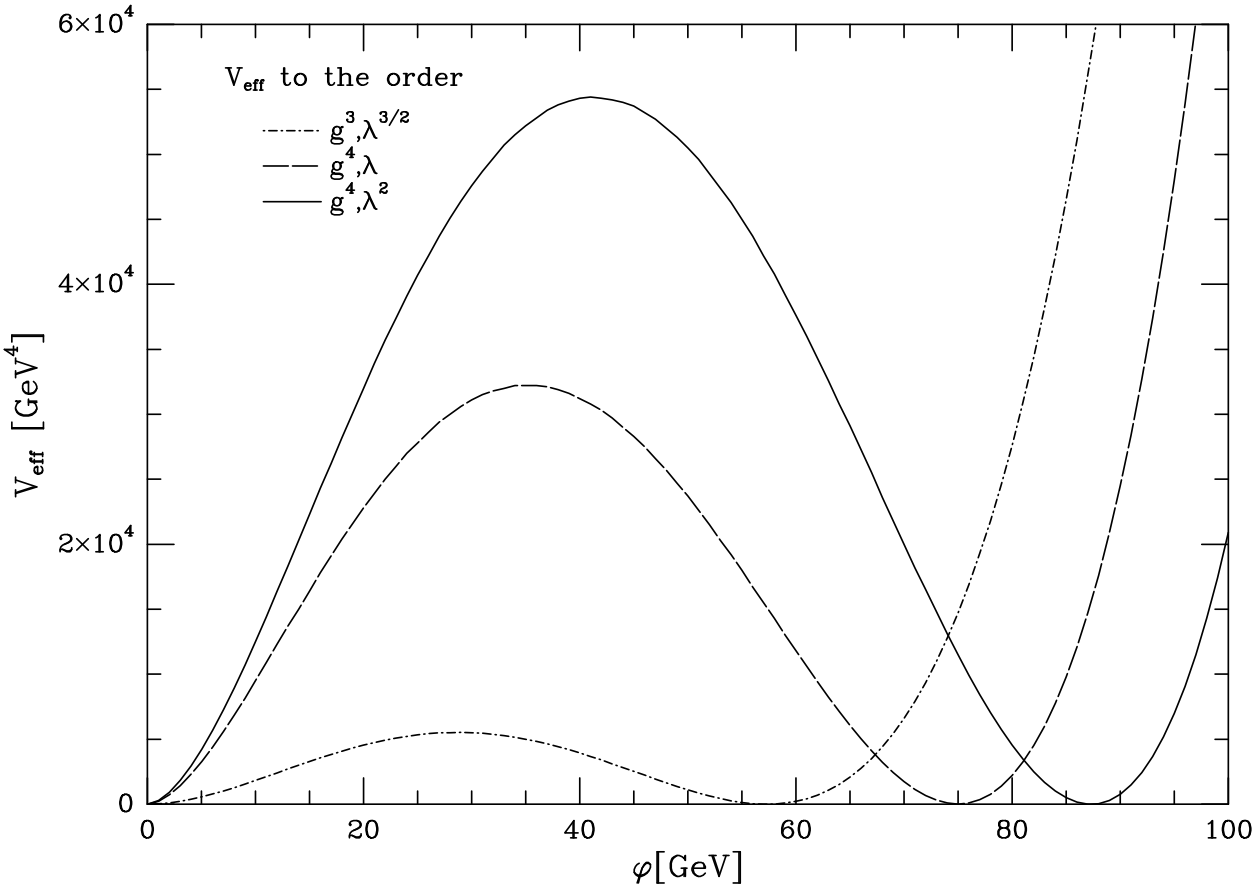

Fig.3 Different approximations of the effective potential plotted at their respective critical temperatures at a Higgs mass of 70 GeV (the g^4, λ-potential is a result of [10])

the one hand the critical temperature and the position of the degenerate minimum seems to be quite stable, on the other hand the hight of the barrier is $\sim$ 10 times larger for the g^4, λ^2 case than for the $g^3, \lambda^{3/2}$-potential. No convergence of the perturbation series can be claimed for the given parameters.

A more detailed picture can be obtained by considering the surface tension [26]

$$\sigma = \int_0^{\varphi_+} d\varphi \sqrt{2V(\varphi, T_c)}, \tag{22}$$

which may be seen as a measure of the strength of the phase transition. It can be used conveniently to discuss the properties of the potential as a function of the Higgs mass. The results are shown in fig. 4. For very small Higgs masses the third order potential gives a much larger value for the surface tension than the more complete calculations. The reason for that is the $g^4\varphi^4$ contribution, which takes over the role of the tree level $\lambda\varphi^4$ term for small scalar coupling. This radiatively induced quartic term ensures that σ does not increase for small Higgs masses, a maximum is found. As could have been expected, corrections of higher order in λ do not change the g^4, λ result if the scalar mass is small.

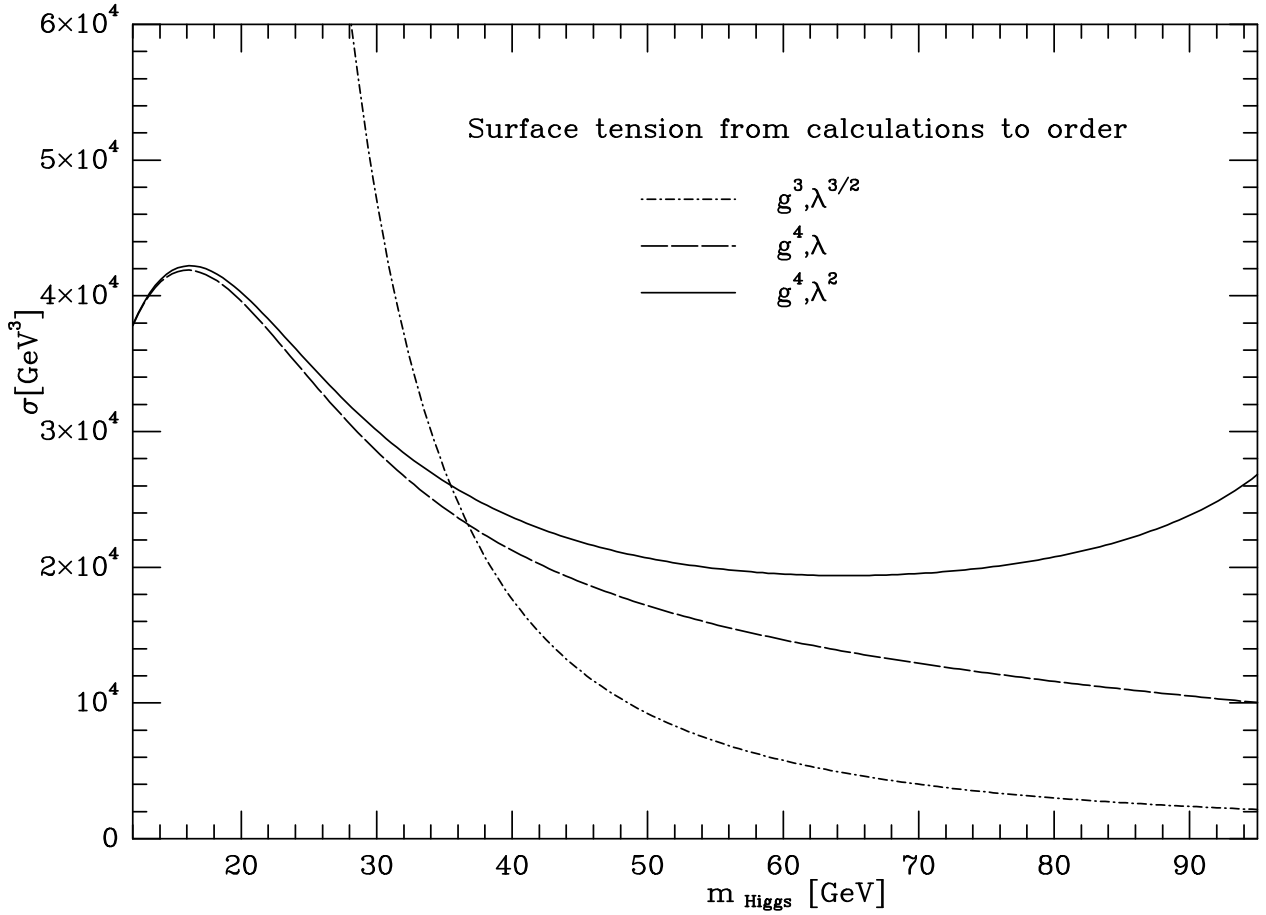

Fig.4 The surface tensions calculated from the different potentials as functions of the zero temperature Higgs mass

This picture changes drastically if larger Higgs masses are considered. In this region higher order corrections produce an enormous increase in the surface tension. The difference between the g^4, λ^2 and the g^4, λ results looks very much the same as in the case of the Abelian Higgs model (see the discussion in [12]). However, in contrast to the situation there in the SU(2)-model both curves suggest much larger values of the surface tension than the $g^3, \lambda^{3/2}$ result.

Let us compare first the results of order $g^3, \lambda^{3/2}$ and g^4, λ^2. The increase in the strength of the phase transition, studied already in [11], can be traced back to the infrared features of a non-Abelian gauge theory. The crucial contribution is the one coming from the non-Abelian setting sun diagram (fig. 2.m). It produces contributions to the potential of type $\varphi^2 \ln(\beta m_W)$ with negative sign. The huge effect of the $\ln \beta m_W$-contribution to the coefficient of $g^4\varphi^2$ can be understood by recalling that at the critical temperature the leading order φ^2-terms essentially cancel. However, the $\varphi^2 \ln \varphi$-type behaviour can not be absorbed in a correction of T_c, these terms increase the strength of the phase transition. The effect becomes

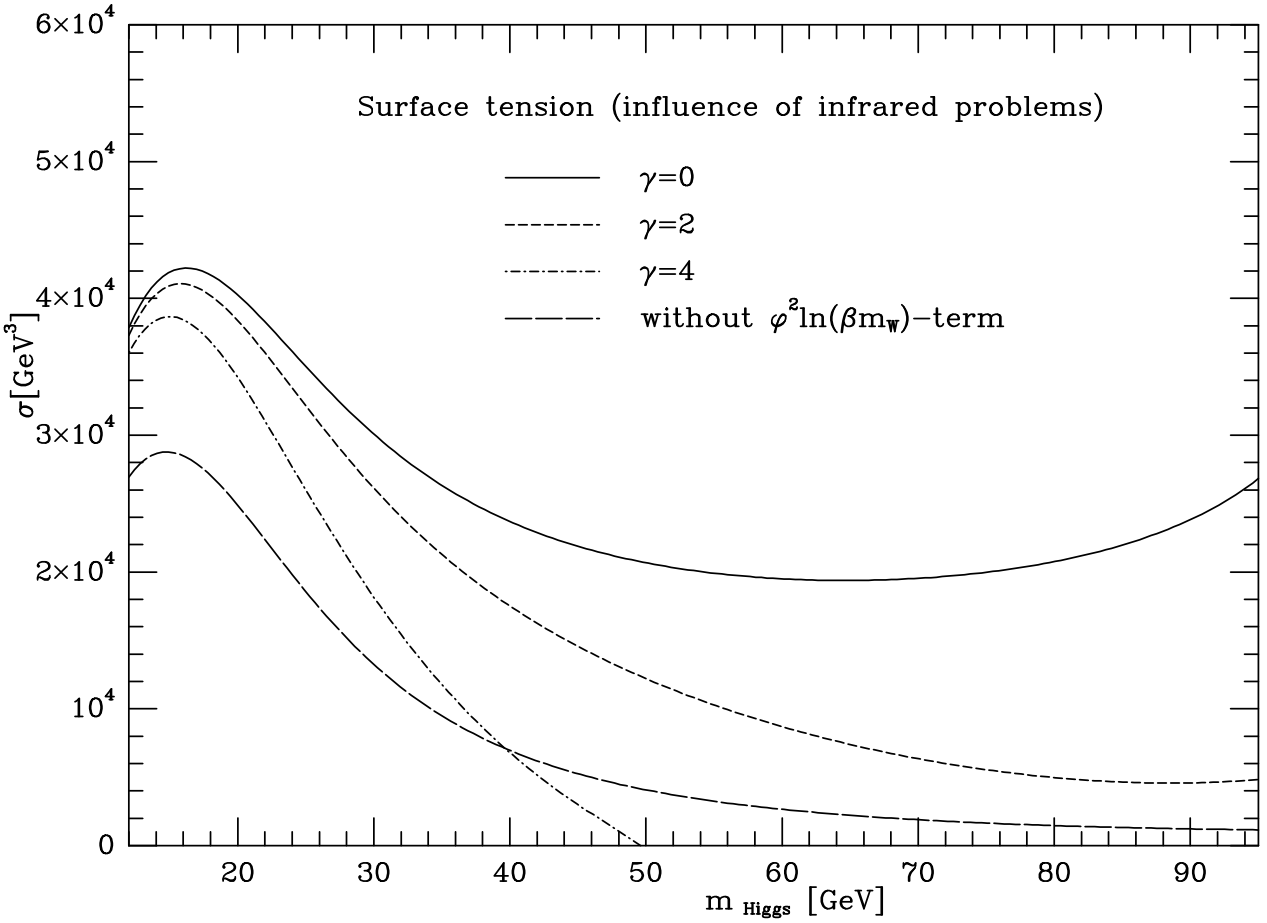

Fig.5 Influence of the most infrared sensitive contributions on the surface tension as a function of the Higgs mass

clear if one deletes the $\varphi^2 \ln \beta m_W$-term of V_m by hand. The corresponding surface tension is shown in fig. 5 (long-dashed line).

We compare now the g^4, λ [10] and the g^4, λ^2 results. The complete calculation produces contributions of type $\varphi^2 \ln \beta(m_W + m_{1,2})$ with positive sign (see appendix). These terms are coming from the scalar-vector setting sun diagrams (fig. 2.a,b). In [10] scalar masses have been neglected, resulting in spurious $\varphi^2 \ln \beta m_W$-terms with positive sign, which reduces the surface tension. Another important contribution is the one proportional to $g^2(m_1+3m_2)m_{WL}$ from V_z. This term comes from scalar-vector diagrams of type of fig. 1.b and it was neglected in [10]. On the relevant scale ($\varphi < T$) it produces a very steep behaviour of the potential, again increasing the surface tension. The observed difference between the result of [10] and the complete g^4, λ^2 calculation presented here is mostly due to these two effects, together with the well known influence of the cubic scalar mass contributions from V_3.

Another interesting effect of higher order λ-corrections is the complete breakdown of the phase transition at a Higgs mass of about 100 GeV, where the surface tension is very

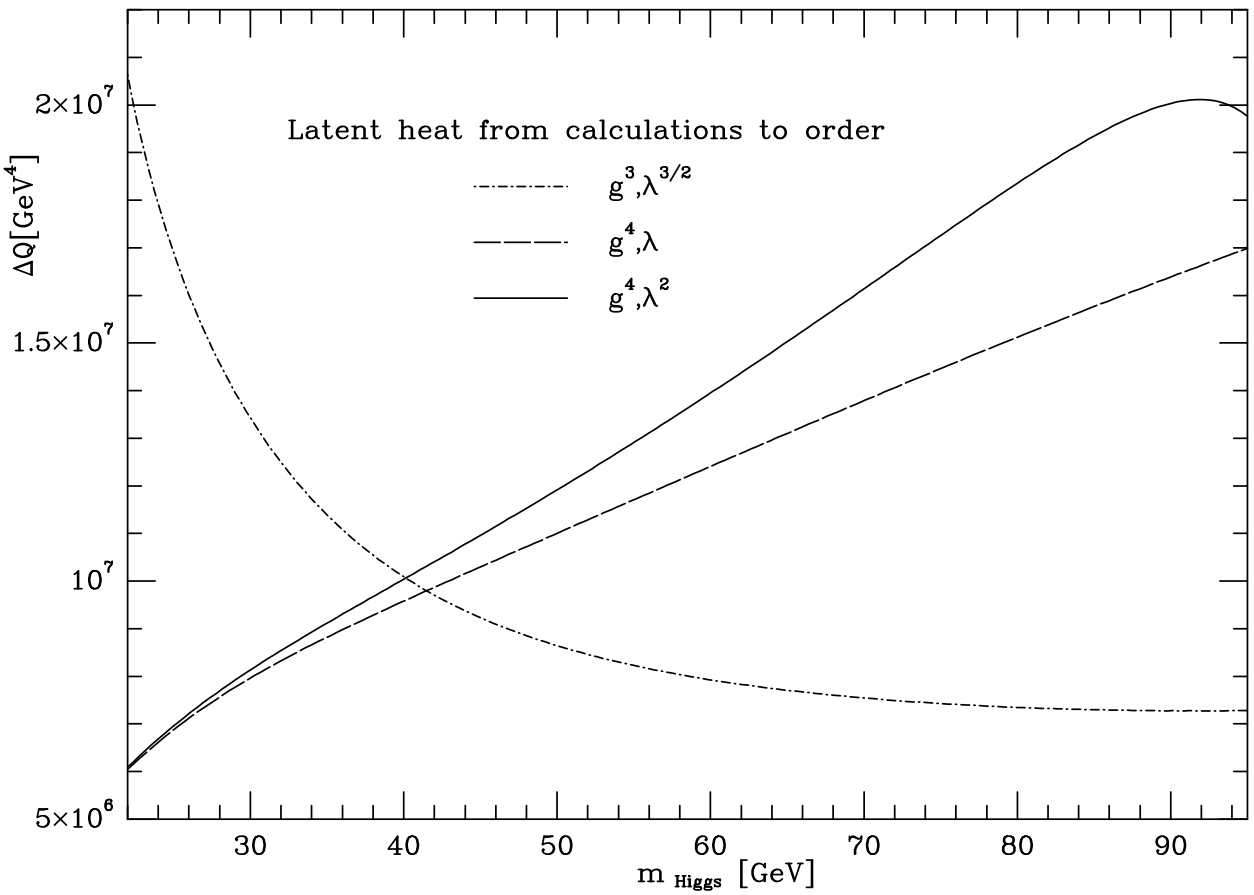

Fig.6 Higgs mass dependence of the latent heat ΔQ of the phase transition

large. In this region the above mentioned term, proportional to $g^2(m_1+3m_2)m_{WL}$, becomes important. For a temperature close to the uncorrected barrier temperature T_b, at which the scalar masses vanish for $\varphi = 0$, it produces an almost linear behaviour in the small φ region. This results in a potential for which at $T = T_b$ the asymmetric minimum is not a global minimum but only a local one. Note that T_b is the lowest temperature accessible in this calculation. In other words, the temperature region in which the phase transition occurs can not be described by the given method, due to infrared problems.

In order to illustrate the possible effects of the unknown infrared behaviour of the transverse vector propagator, the dependence of the surface tension on the magnetic mass can be studied. We follow the approach of [9], where a magnetic mass motivated by the solution of the gap equations was introduced. The transverse vector mass takes the form

$$m_W^2 = \left(\frac{g\varphi}{2}\right)^2 + \left(\frac{\gamma g^2}{3\pi\beta}\right)^2 , \tag{23}$$

where γ is some unknown parameter. One can introduce this redefined transverse mass in the most influential infrared contributions, i.e. in the m_W^3- and in the $\varphi^2 \ln \beta m_W$-terms. We

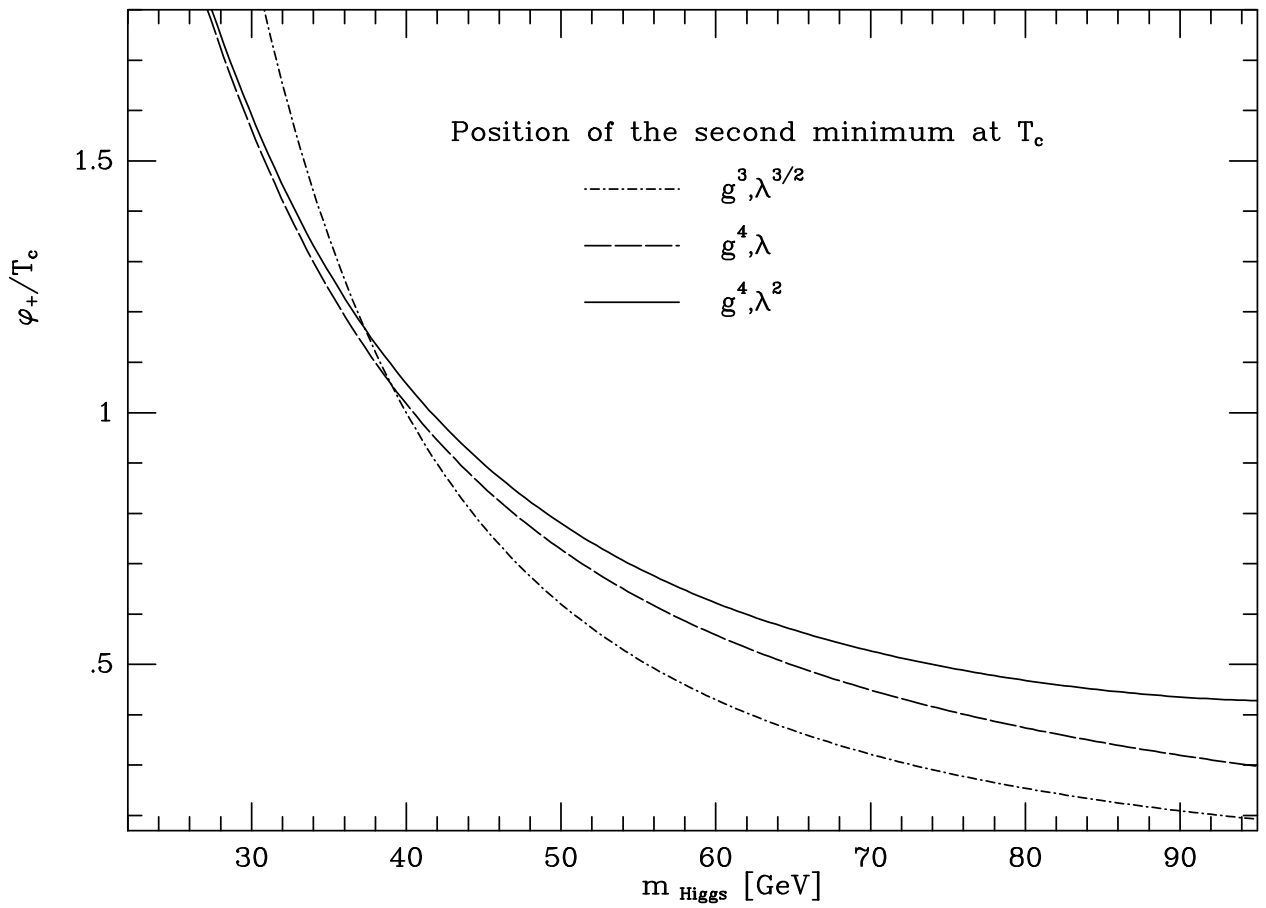

Fig.7 Position of the second minimum φ_+ in units of the critical Temperature T_c

show in fig. 5 the results obtained for $\gamma = 0$, 2 and 4. The qualitative behaviour is similar to results found in [9]. The main difference is due to the fact that the higher order result suggests a stronger first order phase transition, thus for a given $m_{\rm Higgs}$ a larger magnetic mass is necessary to change the phase transition to second order.

A complete fourth order calculation of the surface tension has to include the wave function correction term $Z_\varphi(\varphi^2, T)$ calculated in [18]. Using the results of [18] we have determined σ for Higgs masses between 25-95 GeV. The numerical effect of this Z-factor is very small, only $1\% - 4\%$.

3.2 Further properties of the potential

The latent heat of the phase transition is another interesting quantity to be calculated from the effective potential :

$$\Delta Q = T \frac{\partial}{\partial T} V(\varphi_+, T)\Big|_{T_c}, \tag{24}$$

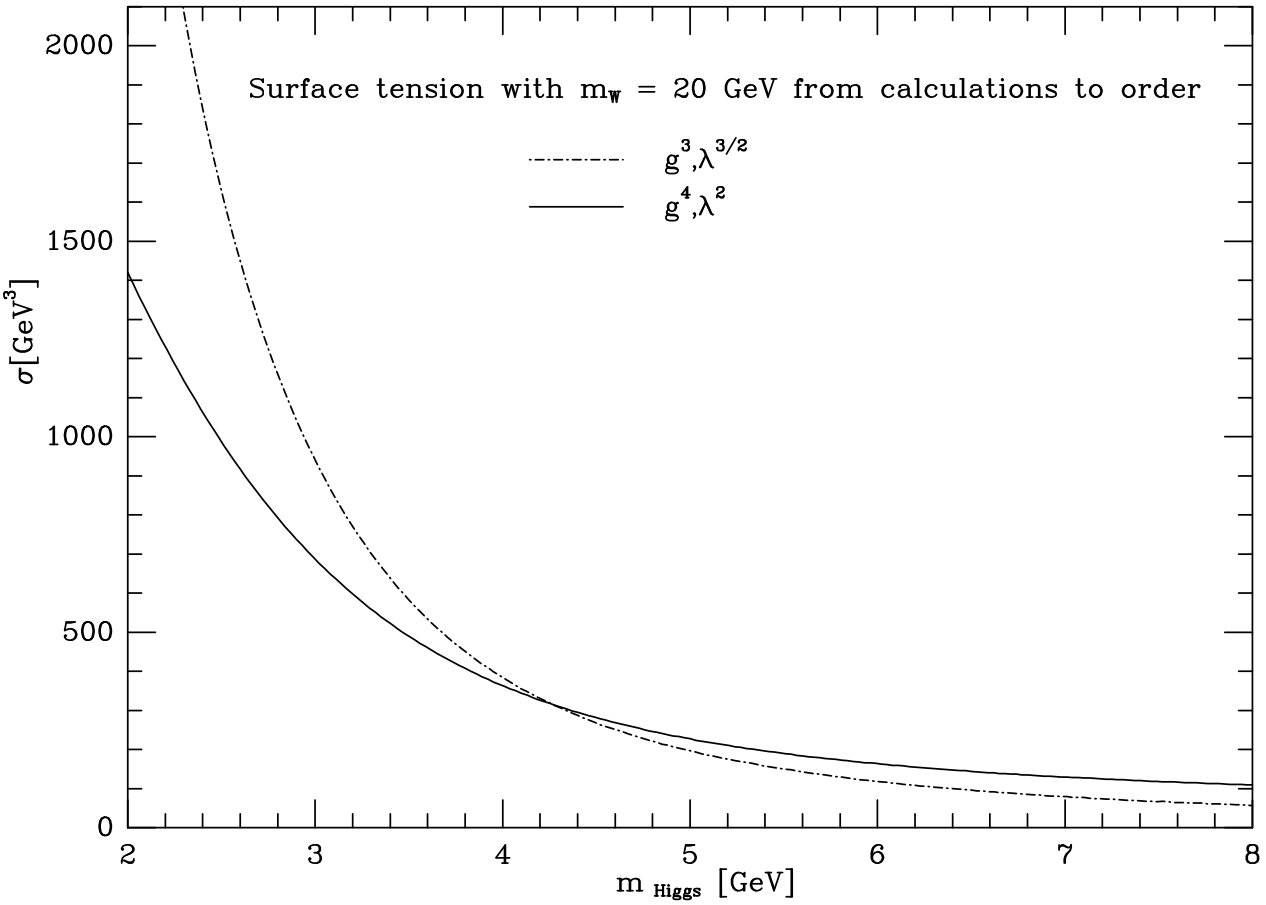

Fig.8 Surface tensions from the third and fourth order potentials for a model with $m_W = 20$ GeV in the Higgs mass range where the values differ by a factor of 2 at most.

where φ_+ is the position of the asymmetric minimum of V. We have plotted ΔQ as a function of $m_{\rm Higgs}$ in fig. 6. The latent heat of the higher order calculations (g^4, λ and g^4, λ^2) increases almost linearly with the Higgs mass. This somewhat surprising behaviour can be understood by observing that for those potentials neither the position of the degenerate minimum nor the height of the barrier change significantly with increasing Higgs mass (see fig. 4). On the other hand the critical temperature is essentially proportional to $m_{\rm Higgs}$.

For completeness, the quantity φ_+/T_c, relevant for baryogenesis, is shown in fig. 7 as a function of the Higgs mass. It is interesting to observe that the upper part of the region favouring baryogenesis [2], i.e. $\varphi_+/T_c \approx 1$ at $m_{\rm Higgs} \approx 40$ GeV, coincides with the region of best reliability of the perturbative approach. As has already been pointed out in [5, 12], this parameter does not reflect the dramatic change of the potential at critical temperature introduced by higher order corrections.

Now the question arises whether a good convergence of the perturbation series, which can not be claimed in the whole range of λ for a realistic gauge coupling $g = 0.64$, could

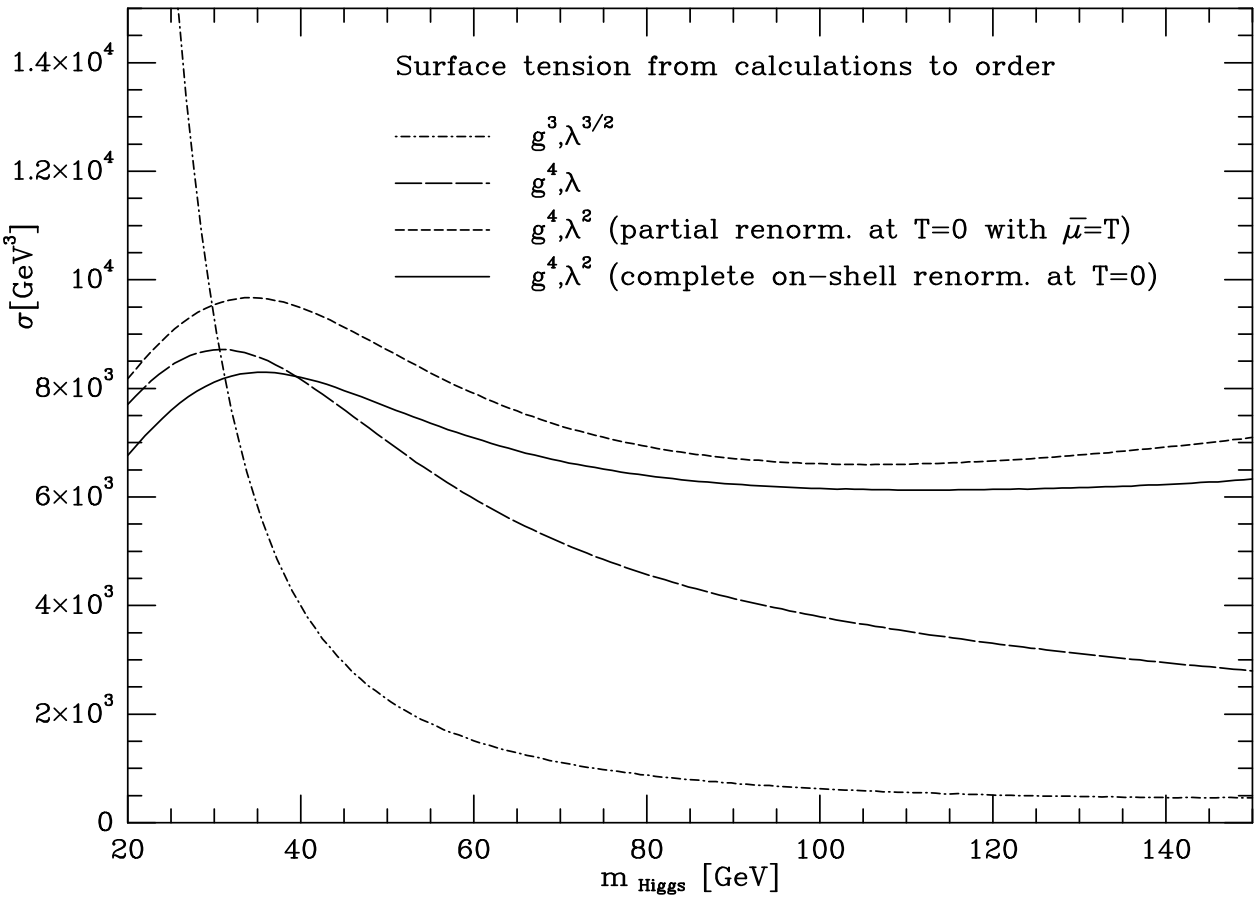

Fig.9 The surface tensions obtained from the standard model effective potentials as functions of the zero temperature Higgs mass with $m_{\rm top} = 140$ GeV

be present in the region of much smaller gauge coupling constants. This seems indeed to be the case, as can be seen in fig. 8, where the surface tensions of order $g^3, \lambda^{3/2}$ and g^4, λ^2 are plotted for a model with a vector mass of 20 GeV, i.e. $g = 0.16$. In the used Higgs mass range the two results for σ differ by a factor of two at most. The relative size of this range, i.e. the ratio of the minimal and maximal values of the Higgs mass, is 4, which is twice as large as the range for the model with $m_W = 80$ GeV.

4 Standard model results

In the case of the full standard model the qualitative behaviour of the potential is essentially the same as for the SU(2)-Higgs model. The main difference is a decrease of the surface tension by a factor ~ 4. This can be traced back to the large top mass. Also the characteristic points of the surface tension plot of fig. 4 are shifted to higher values of the Higgs mass. We show σ as a function of $m_{\rm Higgs}$ in fig. 9. The complete breakdown

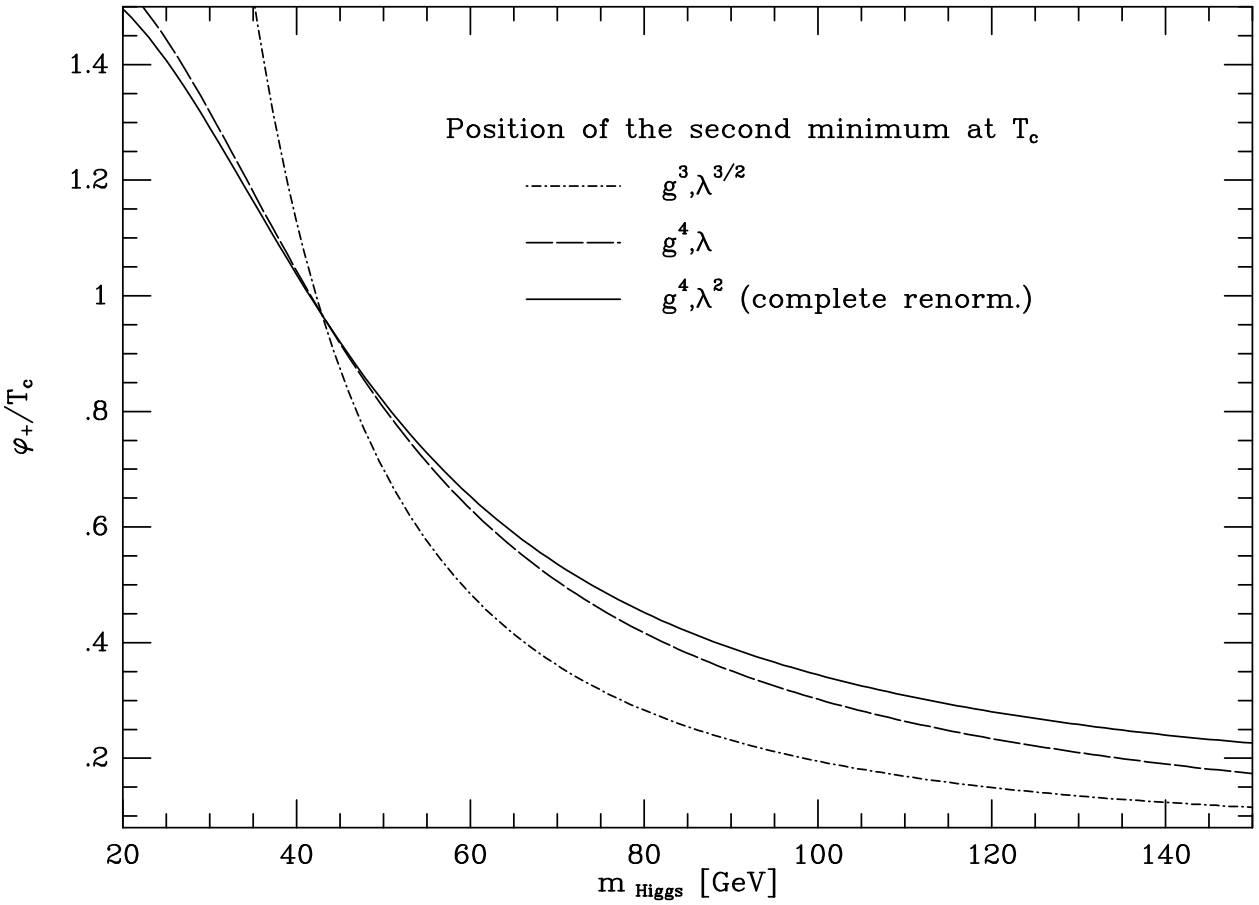

Fig.10 Position of the second minimum φ_+ in units of the critical Temperature T_c in the case of the standard model with $m_{\rm top} = 140$ GeV

of the g^4, λ^2 calculation, observed at $m_{\rm Higgs} \approx 100$ GeV for the pure SU(2) case, occurs at $m_{\rm Higgs} \approx 200$ GeV in the full model. These quantitative differences do not change the qualitative features of the potential, thus the discussion given in the previous section does also apply to the standard model. The difference between the fully renormalized potential and the partially renormalized potential (see eq. (20),(21)) is not too severe in view of the huge uncertainties still present in the perturbative approach. Again, the position of the second minimum at the critical temperature, given in fig. 10, does not depend as strongly on the order of the calculation as the height of the barrier. Unfortunately, the region $m_{\rm Higgs} \approx 40$ GeV, in which the reliability of the perturbative approach is the best and $\varphi_+/T_c \approx 1$, is well below the experimental Higgs mass bound.

5 Conclusions

In the previous sections we have calculated and analyzed the finite temperature effective potential of the standard model up to order g^4, λ^2. We have determined several physical quantities as functions of the Higgs mass. However, to the given order the systematic expansion in coupling constants does not permit a definitive statement about the character of the phase transition for realistic Higgs masses. This is seen from the fact that the g^4, λ^2-corrections are huge and even the step from a g^4, λ-calculation to the complete g^4, λ^2-result changes the potential essentially if the Higgs mass is large. One source of the dramatic increase of the surface tension are the infrared contributions of the typical non-Abelian diagrams. Quantitative information on a possible infrared cutoff, e.g. a magnetic mass term, could increase the reliability of the calculation drastically. For large Higgs masses another infrared problem is connected with the scalar sector, namely the corrected leading order scalar masses vanish near the critical temperature producing an almost linear term in the potential. It has to be concluded, that although resummation techniques permit a systematic expansion in coupling constants, the numerical results still point to the unknown low momentum behaviour of the theory as the main obstacle of any reliable prediction.

Special thanks go to W. Buchmüller for his continuous support of this work. Helpful discussions with D. Bödeker, T. Helbig, B. Kniehl and H. Kohrs are also acknowledged. Z. F. was partially supported by Hung. Sci. Grant under Contract No. OTKA-F1041/3-2190.

Appendix

Here the different contributions to the potential described in sect. 2 are given explicitly. The formulas have been simplified as much as possible to enable a direct numerical use and further analytic investigation. The authors[3] are ready to supply a FORTRAN code evaluating the different approximations of the effective potential ($g^3, \lambda^{3/2}$; g^4, λ; g^4, λ^2 pure $SU(2)$ and standard model, with complete on-shell renormalization or partial renormalization) as a function of φ and T.

Linear mass terms, poles in $2\epsilon = 4 - n$ and terms proportional to the constant ι_ϵ (see [10]), which cancel systematically in the final result, are not shown and the limit $n \to 4$ has

[3]e-mail fodor@vxdesy.desy.de or t00heb@dhhdesy3.bitnet

already been performed. The leading order resummed scalar masses are given by

$$m_1^2 = 2\lambda\varphi^2 + m_2^2 \quad , \quad m_2^2 = \lambda\varphi^2 - \nu + \frac{1}{12\beta^2}\left(6\lambda + \frac{9}{4}g_2^2 + \frac{3}{4}g_1^2 + 3g_Y^2\right) , \tag{25}$$

while the transverse vector boson masses and the fermion mass remain uncorrected to leading order :

$$m_W = \frac{1}{2}g_2\varphi \quad , \quad m_Z = m_W/\cos\theta_W \quad , \quad m_f = \frac{1}{\sqrt{2}}g_Y\varphi\,. \tag{26}$$

The longitudinal SU(2)×U(1) mass matrix receives temperature corrections in the diagonal elements [8]

$$m_{WL}^2 = \frac{1}{4}g_2^2\varphi^2 + \frac{g_2^2}{\beta^2}\left(\frac{5}{6} + \frac{1}{3}n_f\right) \quad , \quad m_{BL}^2 = \frac{1}{4}g_1^2\varphi^2 + \frac{g_1^2}{\beta^2}\left(\frac{1}{6} + \frac{5}{9}n_f\right) , \tag{27}$$

which result in longitudinal masses defined by

$$\begin{pmatrix} m_{WL}^2 & -\frac{1}{4}g_1g_2\varphi^2 \\ -\frac{1}{4}g_1g_2\varphi^2 & m_{BL}^2 \end{pmatrix} = \begin{pmatrix} \cos\tilde{\theta} & \sin\tilde{\theta} \\ -\sin\tilde{\theta} & \cos\tilde{\theta} \end{pmatrix} \begin{pmatrix} m_{ZL}^2 & 0 \\ 0 & m_{\gamma L}^2 \end{pmatrix} \begin{pmatrix} \cos\tilde{\theta} & -\sin\tilde{\theta} \\ \sin\tilde{\theta} & \cos\tilde{\theta} \end{pmatrix} . \tag{28}$$

In the following the short hand notations

$$s = \sin\theta_W \quad , \quad c = \cos\theta_W \quad , \quad \tilde{s} = \sin\tilde{\theta} \quad , \quad \tilde{c} = \cos\tilde{\theta} \tag{29}$$

are used. Evaluating the scalar one- and two-loop temperature integrals the constants

$$c_0 = \tfrac{3}{2} + 2\ln 4\pi - 2\gamma \approx 5.4076 \quad \text{and} \quad c_2 \approx 3.3025 \tag{30}$$

are introduced following [27] and [17] respectively. Now all the contributions to the potential, which have to be summed according to formulas (11) and (17), can be given explicitly :

$$V_3 = \frac{\varphi^2}{2}\left[-\nu + \frac{1}{\beta^2}\left(\frac{1}{2}\lambda + \frac{3}{16}g_2^2 + \frac{1}{16}g_1^2 + \frac{1}{4}g_Y^2\right)\right] + \frac{\lambda}{4}\varphi^4 \tag{31}$$

$$-\frac{1}{12\pi\beta}\left[{m_1}^3 + 3\,{m_2}^3 + 4\,{m_W}^3 + 2\,{m_{WL}}^3 + 2\,{m_Z}^3 + {m_{ZL}}^3 + {m_{\gamma L}}^3\right]$$

$$V_a = \frac{g_2^2}{32\pi^2\beta^2}\left[m_W^2\left(2 - \frac{1}{c^2} + \frac{1}{2c^4}\right)\left(\ln\frac{\beta}{3} - \frac{1}{12}\ln\bar{\mu}^2\beta^2 - \frac{1}{6}c_0 + \frac{1}{4}c_2 + \frac{1}{4}\right)\right. \tag{32}$$

$$\left. + \frac{1}{4}\left(1 + \frac{1}{2c^2}\right)\left\{\left(m_1^2 + 3m_2^2\right)\left(-4\ln\frac{\beta}{3} + \ln\bar{\mu}^2\beta^2 - c_2\right) + 2m_2\left(m_1 + m_2\right)\right\}\right.$$

$$-4s^2m_2^2\ln\left(2m_2\right)-\frac{1}{2m_W}\left(1+\frac{1}{2c}\right)(m_1-m_2)^2(m_1+m_2)+2m_2m_Zs^2$$

$$-\frac{m_W}{2}\left(1+\frac{1}{2c^3}\right)(m_1+3m_2)-\frac{3}{4m_W^2}\left(m_1^2-m_2^2\right)^2\ln(m_1+m_2)$$

$$+\frac{1}{2m_W^2}\left\{m_W^4-2\left(m_1^2+m_2^2\right)m_W^2+\left(m_1^2-m_2^2\right)^2\right\}\ln\left(m_1+m_2+m_W\right)$$

$$+\frac{1}{4m_W^2}\left\{m_Z^4-2\left(m_1^2+m_2^2\right)m_Z^2+\left(m_1^2-m_2^2\right)^2\right\}\ln\left(m_1+m_2+m_Z\right)$$

$$+\left(\frac{1}{4c^2}-s^2\right)\left(m_Z^2-4m_2^2\right)\ln(2m_2+m_Z)+\frac{1}{2}\left(m_W^2-4m_2^2\right)\ln(2m_2+m_W)\Bigg]$$

$$V_b=\frac{g_2^2}{64\pi^2\beta^2}\Bigg[\left\{\left(c^4+\frac{1}{c^4}+4c^2+\frac{4}{c^2}-10\right)m_W^2+2\left(c^2-\frac{1}{c^2}\right)s^2m_2^2+\frac{s^4m_2^4}{m_W^2}\right\} \tag{33}$$

$$\times\ln(m_W+m_Z+m_2)+\left\{\left(5-4c^2\right)m_W^2-\frac{1}{m_W^2}\left(m_W^2c^2+m_2^2s^2\right)^2\right\}\ln(m_W+m_2)$$

$$-\frac{s^4}{m_W^2}\left(m_Z^2-m_2^2\right)^2\ln(m_Z+m_2)+m_W\left\{m_2\left(\frac{1}{c^2}-c^2+\frac{s^4}{c}\right)+m_1\left(1+\frac{1}{2c^3}\right)\right\}$$

$$+m_W^2\left\{\left(\frac{5}{2c^2}+\frac{5}{8c^4}-\frac{5}{4}\right)\left(2\ln\frac{\beta}{9\bar{\mu}}+c_2\right)+\frac{c^2}{2}-\frac{5}{2}+\frac{2}{c^2}+\frac{s^2}{c}\left(c^2-\frac{1}{c^2}\right)\right\}$$

$$-\frac{1}{2m_W^2}\left\{2\left(m_W^2-m_1^2\right)^2\ln(m_W+m_1)+\left(m_Z^2-m_1^2\right)^2\ln(m_Z+m_1)\right\}$$

$$+\left(4m_W^2-2m_1^2+\frac{m_1^4}{2m_W^2}\right)\ln(2m_W+m_1)+\frac{1}{c^2}\left(2m_Z^2-m_1^2+\frac{m_1^4}{4m_Z^2}\right)\ln(2m_Z+m_1)$$

$$+s^2m_2^2\left(2\ln m_2+\frac{s^2}{c}\right)+\frac{m_1^2}{2}\left(1+\frac{1}{2c^2}\right)+\frac{1}{m_W^2}\left(s^4m_2^4\ln m_2+\frac{3}{4}m_1^4\ln m_1\right)$$

$$+\frac{\varphi^2}{4g_2^2}\Big\{(g_2\tilde{c}+g_1\tilde{s})^4\ln(2m_{ZL}+m_1)+(g_2\tilde{s}-g_1\tilde{c})^4\ln(2m_{\gamma L}+m_1)$$

$$+2g_2^4\ln(2m_{WL}+m_1)+2(g_2\tilde{c}+g_1\tilde{s})^2(g_2\tilde{s}-g_1\tilde{c})^2\ln(m_{ZL}+m_{\gamma L}+m_1)$$

$$+4g_2^2g_1^2\left(\tilde{s}^2\ln(m_{WL}+m_{ZL}+m_2)+\tilde{c}^2\ln(m_{WL}+m_{\gamma L}+m_2)\right)\Big\}\Bigg]$$

$$V_i=\frac{1}{8\pi^2\beta^2}\Bigg[\left\{\frac{g_2^2m_f^2}{96}\left(10+\frac{17}{c^2}\right)+\frac{g_2^2n_fm_W^2}{36}\left(\frac{10}{c^2}-\frac{5}{c^4}-14\right)+g_s^2m_f^2\right\} \tag{34}$$

$$\times(\ln\bar{\mu}^2\beta^2-c_0+\frac{1}{2}+\frac{10}{3}\ln 2)-\frac{4g_2^2n_fm_W^2}{27}\left(\frac{10}{c^2}-\frac{5}{c^4}-14\right)\ln 2\Bigg]$$

$$V_j=\frac{g_Y^2}{128\pi^2\beta^2}\left[\left(9m_f^2-m_1^2-3m_2^2\right)\left(\ln\bar{\mu}^2\beta^2-c_0+\frac{3}{2}-\ln 4\right)+48m_f^2\ln 2\right] \tag{35}$$

$$V_m=\frac{g_2^2}{16\pi^2\beta^2}\Bigg[m_W^2\Bigg(\Big(-\frac{1}{4c^4}-\frac{1}{c^2}+\frac{5}{2}-c^2-\frac{c^4}{4}\Big)\ln(m_W+m_Z) \tag{36}$$

$$+\left(\frac{1}{8c^4}+\frac{1}{c^2}-5-4c^2\right)\ln(2m_W+m_Z)+\frac{31}{8}\ln\bar{\mu}^2\beta^2-\frac{11}{16}c_0-\frac{51}{16}c_2-\frac{251}{96}$$

$$-\frac{11}{12}c-\frac{5}{4c}+\frac{1}{8c^2}-4s^2\ln 2+\frac{1}{4}c^2(c-\frac{1}{2})+\frac{1}{8}\left(2-\frac{1}{c^4}\right)\ln c-\frac{51}{4}\ln\frac{\beta}{3}$$

$$+\left(\frac{1}{8c^4}-\frac{23}{4}+5c^2+\frac{1}{4}c^4\right)\ln m_W\Bigg)-m_Wm_{WL}(1+c)-2s^2m_{WL}^2\ln(2m_{WL})$$

$$+\left(\frac{1}{2}m_W^2-2c^2m_{WL}^2\right)\ln(2m_{WL}+m_Z)+\frac{1}{2}m_{WL}^2-\frac{m_{WL}^3}{m_W}$$

$$+\tilde{s}^2\Bigg\{\left(m_W^2-2m_{WL}^2-2m_{\gamma L}^2+\frac{\left(m_{WL}^2-m_{\gamma L}^2\right)^2}{m_W^2}\right)\ln(m_{WL}+m_{\gamma L}+m_W)$$

$$+m_{\gamma L}(m_{WL}-m_W)+\frac{m_{WL}^2m_{\gamma L}+m_{WL}m_{\gamma L}^2-m_{\gamma L}^3}{m_W}-\frac{\left(m_{WL}^2-m_{\gamma L}^2\right)^2\ln(m_{\gamma L}+m_{WL})}{m_W^2}\Bigg\}$$

$$+\tilde{c}^2\Bigg\{\qquad m_{\gamma L}\longrightarrow m_{ZL}\qquad\Bigg\}\Bigg]$$

$$V_p = -\frac{3\lambda^2\varphi^2}{32\pi^2\beta^2}\left[\ln\frac{9\bar{\mu}^2}{\beta^2} - c_2 - 2\ln\{m_1(m_1+2m_2)\}\right] \tag{37}$$

$$V_4 = \frac{\varphi^2}{64\pi^2\beta^2}\Bigg[\frac{g_2^4}{4}\left\{\left(\frac{1}{c^2}-\frac{1}{2c^4}-\frac{35}{4}\right)(\ln\bar{\mu}^2\beta^2 - c_0) + \frac{293}{72} - \frac{1}{18c^2} - \frac{13}{18c^4}\right\} \tag{38}$$

$$+\frac{g_2^4 n_f}{27}\left(\frac{10}{c^2}-\frac{5}{c^4}-14\right) + g_Y^2\left(\frac{g_2^2 s^2}{3c^2} - \frac{3g_Y^2}{4} + 4g_s^2\right)\ln 4 + g_2^2\left(\frac{g_Y^2}{2}+\lambda\right)\left(1+\frac{1}{2c^2}\right)$$

$$+3g_Y^2\lambda\left(\ln\bar{\mu}^2\beta^2 - c_0 + \frac{3}{2}\right)\Bigg] - \frac{1}{64\pi^2}\Big\{-4m_W^4 - 2m_Z^4 - 24m_f^4\ln 4$$

$$+\left(6m_W^4 + 3m_Z^4 + m_1^4 + 3m_2^4 - 12m_f^4\right)\left(\ln\bar{\mu}^2\beta^2 - c_0 + \frac{3}{2}\right)\Big\}$$

$$V_z = \frac{1}{32\pi^2\beta^2}\Bigg[\tfrac{1}{4}(m_1+3m_2)\Big\{g_2^2\left(2m_{WL}+4m_W+m_{ZL}\tilde{c}^2+2m_Z c^2\right) \tag{39}$$

$$+g_1^2\left(m_{ZL}\tilde{s}^2+2m_Z s^2\right) + m_{\gamma L}\left(g_2^2\tilde{s}^2+g_1^2\tilde{c}^2\right)\Big\}$$

$$+\tfrac{1}{2}g_2 g_1(m_1-m_2)\left\{2m_Z sc + (m_{ZL}-m_{\gamma L})\tilde{s}\tilde{c}\right\} + 4g_2^2 m_{WL}\left(m_W + m_Z c^2\right)$$

$$+g_2^2 m_W\left(4m_{\gamma L}\tilde{s}^2 + \tfrac{8}{3}m_W + \tfrac{16}{3}m_Z c^2 + 4m_{ZL}\tilde{c}^2\right) + 3\lambda\left(m_1 m_2 + \tfrac{1}{2}m_1^2 + \tfrac{5}{2}m_2^2\right)\Bigg].$$

References

[1] V. A. Kuzmin, V. A. Rubakov and M. E. Shaposhnikov, Phys. Lett. B155 (1985) 36

[2] A. G. Cohen, D. B. Kaplan and A. E. Nelson, Annu. Rev. Nucl. Part. Sci. 43 (1993) 27

[3] A. Jakovác and A. Patkós, Z. Phys. C60 (1993) 361;
A. Jakovác, K. Kajantie and A. Patkós, preprint HU-TFT-94-01

[4] P. Ginsparg, Nucl. Phys. B170 [FS1] (1980) 388;
J. March-Russel, Phys. Lett. B296 (1992) 364;
M. Gleiser and E. W. Kolb, Phys. Rev. D48 (1993) 1560

[5] P. Arnold and L. G. Yaffe, preprint UW/PT-93-24 (1993)

[6] M. Reuter and C. Wetterich, Nucl. Phys. B408 (1993) 91;
M. Reuter and C. Wetterich, preprint DESY-94-017 and HD-THEP-93-41

[7] B. Bunk, E.-M. Ilgenfritz, J. Kripfganz and A. Schiller, Nucl. Phys. B403 (1993) 453;
K. Kajantie, K. Rummukainen and M. Shaposhnikov, Nucl. Phys. B407 (1993) 356

[8] M. E. Carrington, Phys. Rev. D45 (1992) 2933

[9] W. Buchmüller, Z. Fodor, T. Helbig and D. Walliser, preprint DESY-93-021 (1993), Ann. Phys., to appear

[10] P. Arnold and O. Espinosa, Phys. Rev. D47 (1993) 3546

[11] J. E. Bagnasco and M. Dine, Phys. Lett. B303 (1993) 308

[12] A. Hebecker, Z. Phys. C60 (1993) 271

[13] S. Weinberg, Phys. Rev. D9 (1974) 3357;
D. A. Kirzhnits and A. D. Linde, JETP 40 (1974) 628

[14] C.G. Boyd, D.E. Brahm and S.D.H. Hsu, Phys. Rev. D48 (1993) 4963

[15] J.I. Kapusta, Finite temperature field theory (Cambridge Univ. Press, 1989) pp. 69–72

[16] W. Buchmüller, T. Helbig and D. Walliser, Nucl. Phys. B407 (1993) 387

[17] R.R. Parwani, Phys. Rev. D45 (1992) 4695

[18] D. Bödeker, W. Buchmüller, Z. Fodor and T. Helbig, preprint DESY-93-147 (1993), Nucl. Phys., to appear

[19] M. Böhm, H. Spiesberger and W. Hollik, Fortschr. Phys. 34 (1986) 687

[20] Particle Data Group, K. Hikasa *et al.*, Phys. Rev. D45 (1992) S1

[21] A. Sirlin, Phys. Rev. D22 (1980) 971

[22] G. Degrassi and A. Sirlin, Nucl. Phys. B383 (1992) 73

[23] W. F. L. Hollik, Fortschr. Phys. 38 (1990) 165

[24] F. Jegerlehner, in *Testing the Standard Model—Proceedings of the 1990 Theoretical Advanced Study Institute in Elementary Particle Physics*, ed. by M. Cvetič and P. Langacker (World Scientific, Singapore, 1991) p. 476

[25] W.J. Marciano and A. Sirlin, Phys. Rev. D22 (1980) 2695

[26] S. Coleman, Phys. Rev. D15 (1977) 2929;
A. D. Linde, Nucl. Phys. B216 (1983) 421

[27] L. Dolan and R. Jackiw, Phys. Rev. D9 (1974) 3320